Terahertz two-dimensional high-Q photonic crystal waveguide cavities

A. L. Bingham and D. Grischkowsky*

School of Electrical and Computer Engineering, Oklahoma State University, Stillwater, Oklahoma 74078, USA
**Corresponding author: daniel.grischkowsky@okstate.edu*

Received November 14, 2007; accepted December 23, 2007;
posted January 17, 2008 (Doc. ID 89743); published February 11, 2008

Numerical simulations were used to design a variety of high-Q resonant cavities for integration into a terahertz 2D photonic crystal waveguide. After fabrication, the transmission characteristics of each integrated cavity were explored. These photonic waveguide-coupled cavities demonstrate resonances with linewidths approaching 10 GHz. The results compare favorably to previous observations of rectangular waveguide cavities. Good agreement between the experimental results and the numerical simulations was obtained.

OCIS codes: 130.5296, 130.3120.

Sensing technology is investigating the potential of high-Q resonances for high-sensitivity detection. Devices including microring resonator sensors [1], whispering gallery mode microsensors [2], and corrugated waveguides [3] are made possible owing to the extremely small shifts in either the resonance frequency or the strength of a specific resonance. Owing to this interest, a great deal of terahertz (THz) research has focused on finding ways to generate sharp resonances in an integrated system, typically by placing a defect in an ordered lattice. So far, these defects have been used in a variety of THz waveguide settings, including whispering gallery mode resonators [4], corrugated waveguides [3,5], photonic-crystal-filled waveguides [6,7], and waveguide-coupled resonators [8]. Numerical studies of a photonic crystal waveguide consisting of coupled resonators have demonstrated sensing potential, with the resonant frequency shifting approximately 20 GHz for index variations on the order of 2% [9]. In the sub-THz region (100 GHz) a dielectric photonic crystal waveguide was utilized as a sensor by filling the air holes with liquids [10].

At the same time, integrated 2D channels have been demonstrated in a photonic crystal waveguide at THz frequencies [11]. This waveguide demonstrated attenuation approximately equal to or even less than that of a comparable rectangular waveguide over much of the 0–4 THz experimental bandwidth. In addition to its favorable propagation characteristics, the photonic crystal waveguide has potential as a platform for integrated components. Thus far, photonic crystal waveguides have not been used to generate sharp THz resonances. However, photonic crystals have three distinct advantages as a base for cavity design. First, photonic crystals are capable of extremely high confinement. Second, it is simple to integrate cavities into photonic crystal waveguides by breaking the periodicity at certain points, i.e., removing individual cells of the lattice. Third, by using numerical techniques, it is possible to accurately design photonic crystal cavities with specified sharp resonances.

This letter describes the design, fabrication, and experimental verification of photonic crystal waveguide cavities to create sharp resonances. Four photonic crystal waveguides, each with a different integrated cavity, are demonstrated and show different resonances of varying strength and sharpness. These experimental data are then compared to 2D finite-difference time-domain (FDTD) simulations.

Before fabricating the photonic crystal cavities, a variety of different designs were simulated using an FDTD method [12]. After simulations, the waveguide-coupled cavities with the sharpest resonant lines were chosen for fabrication. Scanning electron microscope (SEM) images of the different waveguide geometries are shown in Fig. 1. The slight remaining surface structure, where the cavity has been cut, is subwavelength and has minimal effect on the transmission through the waveguides. WG-1 (not shown) is the reference waveguide with no cavity; coupled cavities WG-2–WG-5 are presented. The WG-2 cavity has been formed by simply removing a single cylinder in the waveguide sidewall. The WG-3 cavity is similar to WG-2 with one additional cylinder removed. WG-4 and WG-5 have a larger 3×1 cavity,

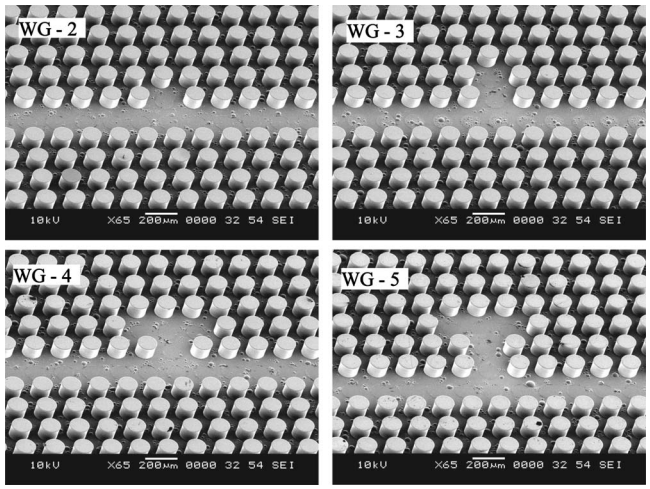

Fig. 1. SEM images of the four waveguide coupled cavities.

0146-9592/08/040348-3/$15.00

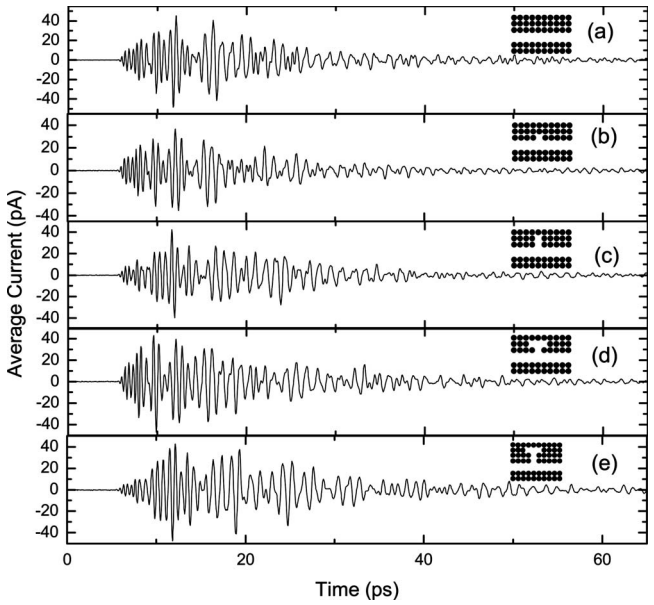

Fig. 2. Output THz pulses from (a) WG-1, (b) WG-2, (c) WG-3, (d) WG-4, and (e) WG-5.

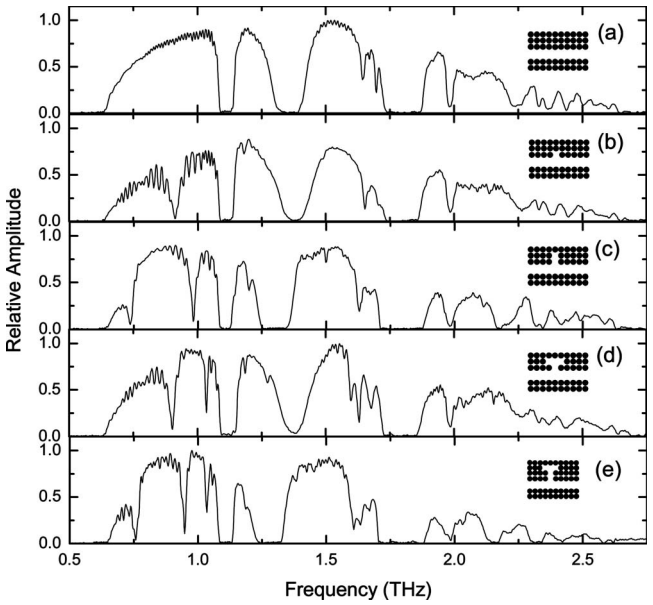

Fig. 3. Normalized amplitude spectrum of (a) WG-1, (b) WG-2, (c) WG-3, (d) WG-4, and (e) WG-5.

which is displaced from the waveguide channel by either one or two cylinders, respectively. All of the cavities produce sharp THz resonances in the first passband of the waveguide.

The fabrication of the photonic crystal lattice follows a procedure similar to what has been previously published [13]. The crystal lattice consists of 70 μm tall, 108 μm diameter cylinders with a period of 160 μm. It should be noted that these cylinders have a $\sim$40 μm larger diameter than for the previous waveguide demonstration [11]. This lattice was patterned onto a wafer, which was diced into a 25.4 mm wide$\times$9.43 mm long photonic chip. The five separate waveguide channels, four with different coupled cavities, were then cut into the lattice by hand with a tungsten dissecting probe. Each waveguide channel was separated on each side by a minimum of 15 rows, or 2.4 mm, ensuring that there was no cross talk between channels. After cutting the channels through the photonic crystal lattice, the chip was metallized with 400 nm of gold and placed into a matched 9.43 mm long aluminum parallel plate waveguide. The waveguide was then placed in the confocal beam waist of a standard THz-TDS system [14]. Two hyperhemispherical silicon lenses are used to couple the THz beam into and out of the waveguide [15].

Time-domain data were then taken for each of the five waveguides in sequential order. After data for one waveguide cavity were taken, the silicon lenses were moved back, and the waveguide holder was vertically displaced to the next waveguide cavity. The lenses were then brought back into contact with the waveguide, and the process was repeated. Figures 2(a)–2(e) show the THz pulses transmitted through each of the five waveguides. For purposes of illustration, the pulses are only shown to 65 ps, although the measured ringing cleanly extends to 130 ps until the arrival of reflections from the silicon lenses. Scans longer than 130 ps were also taken to ensure that the resonances were completely resolved, but the resonance's strength and linewidth did not vary. All five pulses show significant broadening due to propagation through the 9.43 mm long dispersive photonic crystal cavity waveguides [9,15].

The Fourier-transformed output spectra for the four cavity waveguides are shown in Fig. 3. Each of the output spectra has been normalized to WG-1. While the spectrum from WG-1 is similar to the previous demonstration of a photonic crystal waveguide [11], the subsequent waveguides (each with a different coupled cavity) all have additional sharp resonant lines. While there are a number of sharp features in each of the spectra, the focus here will be on resonances in the first passband, where the transmission is cleanest. The relatively simple cavity of WG-2 has a line at 0.914 THz, with an approximate FWHM power linewidth of 42 GHz. WG-3 has two sharp resonances at 0.737 and 0.982 THz with corresponding FWHMs of 18 and 37 GHz. WG-4 has resonances at 0.903 and 1.034 THz with corresponding FWHMs of 24 and 13 GHz. The most complex cavity, WG-5, has resonances at 0.757, 0.948, and 1.034 THz with corresponding FWHMs of 26, 22, and 16 GHz. These values are considered accurate to ±3 GHz. In addition, all of the coupled-cavity waveguides show sharp oscillations in the first passband, which are not present in the reference waveguide. These oscillations result from internal reflections due to the insertion of a cavity into the waveguide.

Figure 4 shows the comparison of simulation (solid curve) and experiment (dashed curve with dots) for WG-4 in the first passband. The simulations were performed with matching geometrical parameters but with perfectly conducting cylinders [12]. The transmitted output pulse was calculated in the 2D plane with 5 μm steps to a 130 ps temporal extent. The amplitude Fourier transform of this calculated pulse is shown in Fig. 4. Similar results were obtained with 2 μm steps. The simulated spectrum has

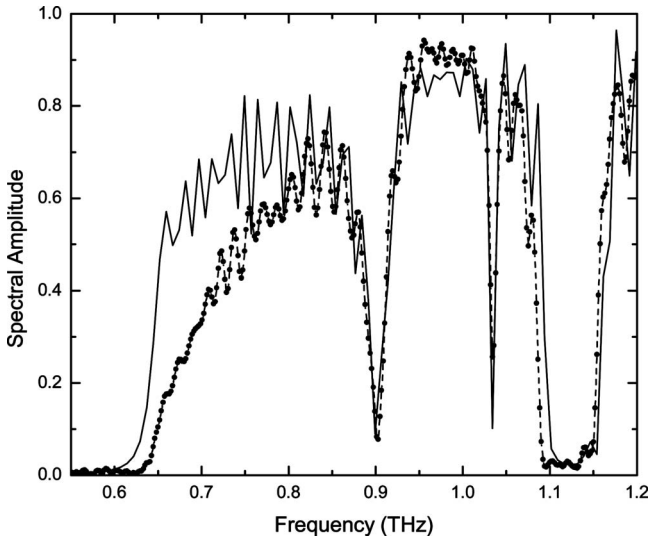

Fig. 4. Comparison of amplitude spectra of the FDTD simulation (solid curve) and experimental output (dashed curve with dots) from WG-4 in the first passband.

been linearly scaled to match the experimental spectrum. The match between the two spectra is excellent for the resonant lines at 0.903 and 1.034 THz. The perfect conductivity of the cylinders in the simulation allows longer pulse ringing, as shown by the sharp oscillations between 0.65 and 0.9 THz. These oscillations develop in the experimental spectrum as the frequency increases above the cutoff frequency, where the absorption is highest.

The resonant cavity frequencies, v_o, and the power FWHM linewidths, Δv, for all of the experimental results are compared to the numerical simulations in Table 1. The linewidths include both cavity and coupling loss [8]. The match between the theory and experiment is again excellent, as all of the resonant frequencies for the simulations match the experimental resonant frequencies to within 10 GHz. Additionally, the experimental linewidths are in good agreement with the slightly sharper simulated linewidths, as the infinite conductivity of the cylinders in the simulation allows longer cavity lifetimes. The strong overlap between numerical simulations and the experiment allows an accurate design for future experiments and applications.

Table 1. Comparison of v_o and Δv for the Experimental Results and the Numerical Simulations of the Different Cavities; These Values Are Considered Accurate to ±3 GHz

Waveguide	ν_O (THz)	$\Delta\nu$ (GHz)	FDTD ν_O (THz)	FDTD $\Delta\nu$ (GHz)
WG-2	0.914	42	0.915	42
WG-3	0.737	18	0.736	14
WG-3	0.982	37	0.986	33
WG-4	0.903	24	0.902	20
WG-4	1.034	13	1.0350	10
WG-5	0.757	26	0.763	25
WG-5	0.948	22	0.951	25
WG-5	1.034	16	1.044	11

The resonances in the photonic crystal waveguide cavities are notably sharper than the previously demonstrated traditional cavities in a rectangular waveguide, which had typical FWHM linewidths of 50 GHz [8]. This is especially interesting as the photonic crystal waveguides have sharper lines despite having significantly larger apertures. For comparison, the aperture of the photonic crystal cavities is a minimum of ~210 μm wide. For the rectangular waveguide cavities, the aperture is 110 μm wide, almost twice as small. Additionally, the photonic crystal boundary lacks the complete metallic boundary on the sidewalls of the cavity.

We have demonstrated cavities with sharp resonances coupled to a THz 2D photonic crystal waveguide. The more complex cavities produced sharper resonances, which vary in FWHM linewidths from 13 to 42 GHz. The numerical simulations provide an excellent match for the experimental results. When compared to previous work involving traditional THz rectangular waveguides with side-coupled resonators, the photonic cavity resonances are up to four times sharper. It is expected that even sharper resonances could be observed as more advanced cavities are developed. These integrated photonic cavities represent the first of many potential integrated devices within the THz photonic crystal waveguide.

This work was partially supported by the National Science Foundation.

References

1. C.-Y. Chao and L. J. Guo, J. Vac. Sci. Technol. B **20**, 2862 (2002).
2. J. Nadeau, V. Ilchenko, D. Kossakovski, G. Bearman, and L. Maleki, Proc. SPIE **4629**, 172 (2002).
3. M. Nagel and H. Kurz, Int. J. Infrared Millim. Waves **27**, 517 (2006).
4. J. Zhang and D. Grischkowsky, J. Opt. Soc. Am. B **20**, 1894 (2003).
5. A. L. Bingham and D. Grischkowsky, Appl. Phys. Lett. **90**, 091105 (2007).
6. Z. Jian, J. Pearce, and D. M. Mittleman, Opt. Lett. **29**, 2067 (2004).
7. Y. Zhao and D. R. Grischkowsky, IEEE Trans. Microwave Theory Tech. **55**, 656 (2007).
8. P. George, C. Manolatou, F. Rana, A. Bingham, and D. Grischkowsky, Appl. Phys. Lett. **91**, 191122 (2007).
9. H. Kurt and D. S. Citrin, Appl. Phys. Lett. **87**, 241119 (2005).
10. T. Hasek, H. Kurt, D. S. Citrin, and M. Koch, Appl. Phys. Lett. **89**, 173508 (2006).
11. A. L. Bingham and D. Grischkowsky, IEEE Microw. Wirel. Compon. Lett. (2007), accepted for publication.
12. M. Qiu, F2P: finite-difference time-domain 2D simulator for photonic devices, http://www.imit.kth.se/info/FOFU/PC/F2p/
13. A. Bingham, Y. Zhao, and D. Grischkowsky, Appl. Phys. Lett. **87**, 051101 (2005).
14. M. van Exter and D. Grischkowsky, IEEE Trans. Microwave Theory Tech. **38**, 1684 (1990).
15. G. Gallot, S. P. Jamison, R. W. McGowan, and D. Grischkowsky, J. Opt. Soc. Am. B **17**, 851–863 (2000).